Phosphonate removal from discharged circulating cooling water using iron–carbon micro-electrolysis

Zhen Zhou, Weimin Qiao, Yangbo Lin, Xuelian Shen, Dalong Hu, Jianqiao Zhang, Lu-Man Jiang and Luochun Wang

ABSTRACT

Phosphonate is a commonly used corrosion and scale inhibitor for a circulating cooling water (CCW) system. Its discharge could cause eutrophication of receiving waters. The iron–carbon (Fe/C) micro-electrolysis technology was used to degrade and remove phosphonate from discharged CCW. The influences of initial pH, Fe/C ratio (FCR) and temperature on phosphonate removal were investigated in a series of batch tests and optimized by response surface methodology. The quadratic model of phosphonate removal was obtained with satisfactory degrees of fitness. The optimum conditions with total phosphorus removal efficiency of 95% were obtained at pH 7.0, FCR of 1.25, and temperature of 45 °C. The phosphonate removal mechanisms were also studied. Phosphonate removal occurred predominantly via two consecutive reactive phases: the degradation of phosphonate complexes (Ca–phosphonate) and the precipitation of Fe/C micro-electrolysis products (PO_4^{3-}, Ca^{2+} and Fe^{3+}).

Key words | circulating cooling water, iron–carbon micro-electrolysis, phosphonate, response surface methodology

Zhen Zhou (corresponding author)
Weimin Qiao
Yangbo Lin
Xuelian Shen
Dalong Hu
Jianqiao Zhang
Lu-Man Jiang
Luochun Wang
College of Environmental and Chemical Engineering,
Shanghai University of Electric Power,
Changyang Rd #2588,
Shanghai 200090,
China
E-mail: *zhouzhen@shiep.edu.cn*

INTRODUCTION

In China 50–80% of the water consumed in thermoelectric power production is used as circulating cooling water (CCW), of which approximately 20–30% is directly discharged into sewerage systems (Kenny *et al.* 2009). Phosphonate-based corrosion and scale inhibitors are commonly used in CCW systems to prevent scale formation and metal corrosion (Demadis *et al.* 2006, 2008; Akyol *et al.* 2009). After accumulating, total phosphorus (TP) in the discharged CCW may exceed 3 mg/L. With such large flow rate and such concentration, phosphorus in CCW is considered to be a potential cause of the eutrophication of receiving waters (Le *et al.* 2010). Therefore, the removal of phosphorus from CCW becomes one of the important targets for power plants to meet more and more stringent standards for nutrient pollutants discharge.

Enhanced biological phosphorus removal and chemical precipitation are the two conventional methods applied for phosphorus removal (Wang *et al.* 2009). Biological methods are not suitable for CCW because the biocide agents and high salinity in the CCW would inhibit microbial activity. Moreover, the chelating property and stability of the phosphonate also prevent its precipitation with such metal precipitators as ferric, aluminum, calcium and magnesium salts (Marín-Cruz *et al.* 2007). Therefore, alternative removal methods have to be investigated.

A feasible way to remove phosphorus from CCW is by degrading phosphonate to orthophosphate, which is easier to precipitate with metals. The degradation and precipitation could be achieved simultaneously by iron–carbon (Fe/C) micro-electrolysis method owing to its good performances in adsorption, flocculation and co-precipitation (Pan *et al.* 2011; Guo *et al.* 2013). This method has been widely used in the treatment of coking, dyeing, pesticide, pharmaceutical and chemical wastewater (Cheng *et al.* 2007; Le *et al.* 2011; Liang *et al.* 2012) because of its advantages of easy operation, low cost and high efficiency.

The objective of this work was to study the feasibility of using Fe/C micro-electrolysis method for phosphonate removal from discharged CCW. The effects of pH, Fe/C ratio (FCR) and temperature on phosphorus removal were evaluated using batch tests with real CCW. The Box–Behnken design for response surface methodology (RSM)

doi: 10.2166/wst.2014.248

was applied to optimize the operating conditions. The results obtained in this study will provide useful information on using Fe/C micro-electrolysis method as an alternative way for phosphonate removal from discharged CCW.

METHODS

Materials

The iron filings were procured from a mold factory in Shanghai, China. The materials were passed through a 2 mm sieve, and then treated by 5% hot NaOH solution to remove oil film from the surface. Activated carbon (AC) with particle size of 1–2 mm was washed with tap water. Both iron filings and AC were dried at 100 °C. The discharged CCW used in this study was collected from Wujing Power Plant in Shanghai, China. 1-Hydroxyethane-1-1-diphosphonic acid (HEDP) was employed as a corrosion and scale inhibitor of the CCW, and the phosphonate, orthophosphate phosphorus (PO_4-P) and phosphite phosphorus (PO_3-P) contents were 7.90%, 0.05% and 0.25%, respectively.

Batch experimental procedure

Batch experiments of Fe/C micro-electrolysis were performed to determine the influence of important operating parameters such as FCR, initial pH and temperature of the wastewater on TP removal of the discharged CCW. Six FCRs (0.5, 0.75, 1.0, 1.25, 1.75 and 2.0) were used to study the effect of FCR on phosphonate removal of CCW. The pH and temperature were maintained at initial pH of the discharged CCW (8.8 ± 0.2) and 20 ± 1 °C, respectively. The dosage of iron and AC was about 160 mL/L. All samples were shaken at 50 rpm for 120 min. Six initial pH values (4.0, 5.0, 7.0, 8.0, 9.0 and 10.0) were chosen to evaluate the effect of pH on phosphonate removal with 250 mL of CCW sample under FCR of 1.0. Six temperatures (15, 25, 35, 40, 45 and 50 °C) were used to evaluate the effect of temperature on phosphonate removal. The initial pH value was maintained at 8.8 ± 0.2 for the batch test.

Box–Behnken experimental design

As a statistical technique for modeling and analysis, RSM has been used to solve problems in which a response of interest is influenced by several factors. The Box–Behnken design is used to optimize the effective parameters, as well as to analyze the relationships between the parameters. The relationship between the response variables and the set of parameters is given in Equation (1)

$$Y = \beta_0 + \sum_{i=1}^{k} \beta_i X_i + \sum_{i=1}^{k} \beta_{ii} X_i^2 + \sum_{i=1}^{k} \sum_{j=1}^{k} \beta_{ij} X_i X_j + \varepsilon \quad (1)$$

where Y is the response variable; β_0 is the constant term; k is the number of factors; β_i, β_{ii} and β_{ij} are coefficients of the first order terms, quadratic terms and interaction terms, respectively, while ε is the residual associated with the experiment (Myers & Anderson-Cook 2009).

Based on the single factor tests, the three-factor three-level Box–Behnken experimental design was used to investigate and validate reaction parameters affecting phosphonate removal by Fe/C micro-electrolysis. FCR (X_1: 0.5–2.0), pH (X_2: 7.0–10.0) and temperature (X_3: 10–45 °C) were selected as the three factors, and TP removal efficiency (PR) (Y) was selected as the response variable. The selected ranges of respective parameters, coded as −1 (low), 0 (middle), and +1 (high) (Tripathi *et al.* 2009), are given in Table 1. The

Table 1 | The design matrix based on coded and real variables for experimental factors and response

	Real values of variables			
Test	**X_1 (pH)**	**X_2 (FCR)**	**X_3 (Temperature)**	**PR efficiency (%)**
Low (−1)	7	0.5	15	–
Middle (0)	8.5	1.25	30	–
High (1)	10	2	45	–
1	8.5	1.25	30	85.68 ± 0.34
2	10	2	30	85.79 ± 0.41
3	7	0.5	30	75.03 ± 0.23
4	8.5	1.25	30	81.12 ± 0.45
5	8.5	1.25	30	83.59 ± 0.20
6	8.5	2	45	86.89 ± 0.26
7	8.5	1.25	30	81.87 ± 0.33
8	7	1.25	15	60.15 ± 0.37
9	10	1.25	45	92.98 ± 0.29
10	8.5	0.5	45	82.79 ± 0.40
11	8.5	1.25	30	85.68 ± 0.34
12	7	1.25	45	92.81 ± 0.41
13	10	0.5	30	80.96 ± 0.18
14	10	1.25	15	92.98 ± 0.29
15	8.5	0.5	15	59.53 ± 0.25
16	8.5	2	15	77.77 ± 0.27
17	7	2	15	84.61 ± 0.31

experimental data were analyzed by Design Expert software version 8.0.6.1 for regression analysis and model development.

Analysis method

Chemical oxygen demand (COD), TP and PO_4-P were determined according to Chinese standard methods (Chinese NEPA 2012). The pH and conductivity were determined by an HQd portable tester (Hach, USA). The turbidity was determined by a 2100Q turbidity meter (Hach, USA). The morphology and elemental composition of the solid materials (iron and AC) were observed with SU-1500 (Japan) scanning electron microscopy (SEM) at 25.0 kV, coupled with energy-dispersion spectroscopy (EDS).

RESULTS AND DISCUSSION

Characteristics of the discharge CCW

The pH of discharged CCW was 8.8 ± 0.2. Average conductivity and turbidity were 2024 ± 1 μS/cm and 8.2 ± 0.9 NTU, respectively. The average COD, TP and concentration of PO_4-P in the CCW were 16.7 ± 1.6, 2.51 ± 0.07 and 0.10 ± 0.01 mg/L, respectively. The low proportion of PO_4-P in the TP (4.0%) indicated high stability of phosphonate in the discharge CCW, which could prevent the precipitation of phosphorus with metal precipitators.

Effect of initial pH on phosphonate removal

The effect of pH on phosphonate removal at FCR of 1.0 and temperature of 20 ± 1 °C is demonstrated in Figure 1(a). PR value was found the lowest at pH 7.0. The PR decreased from 75.4% to 61.5% when pH changed from 4.0 to 7.0. Then it increased to 73.0% when pH reached 9.0. A slight decrease of PR was observed at pH 10.0 (72.1%).

The results showed that pH had a distinct effect on phosphonate removal by Fe/C micro-electrolysis in acidic and alkaline conditions. In the acidic condition, lower pH caused stronger electrolytic reaction activity on the iron surface, and more nascent hydrogen ([H]) and Fe^{2+} (oxidized to Fe^{3+} by dissolved oxygen rapidly) were released during the micro-electrolysis process. Furthermore, phosphonate was decomposed to orthophosphate by active ingredients, and

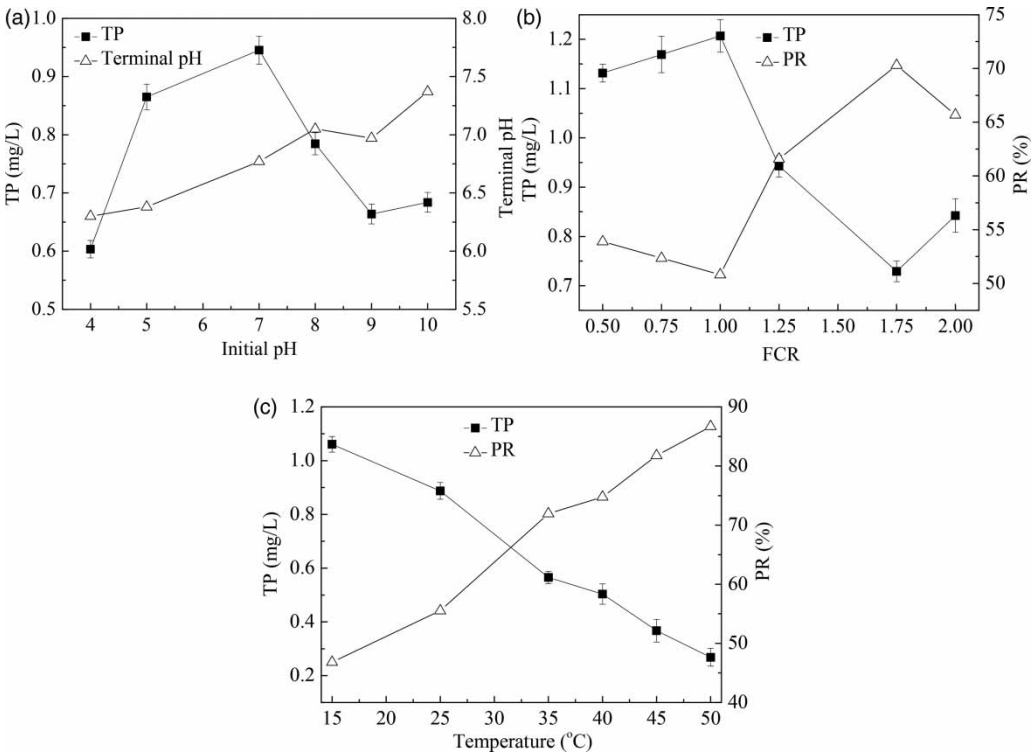

Figure 1 | Effect of (a) pH, (b) FCR and (c) temperature on phosphonate removal from discharged CCW.

then a reaction as Equation (2) may occur and lead directly to the phosphorus removal

$$Fe^{3+} + PO_4^{3-} \rightarrow FePO_4 \downarrow \quad (2)$$

In the alkaline condition, electrolytic reaction between iron and active carbon would produce hydroxyl group, which is an important part of $Fe(OH)_2/Fe(OH)_3$ colloid. The existence of $Fe(OH)_2/Fe(OH)_3$ in solution would increase the organic and inorganic phosphorus removal by flocculation or adsorption. As shown in Figure 1(a) pH values of all tests tended to be neutral after reaction, which indicated that both H^+ and OH^- participated in phosphonate removal. Considering the initial pH of the discharge CCW was 8.8 ± 0.2, a higher PR could be achieved (about 72% in Figure 1(a)) without regulating pH in this study.

Effect of FCR on phosphonate removal

Iron corrosion was enhanced by combining with AC acting as a micro-cathode. The effect of FCR on phosphonate removal is shown in Figure 1(b). The PR decreased slightly with FCR increasing from 0.5 to 1.0, and then was significantly enhanced by further increasing the ratio to 1.75. With the FCR increasing from 1.75 to 2.0, the PR decreased from the maximum value of 70.3% to 65.7%. At low FCR, excessive AC might block the contact between iron and dissolved oxygen/H_2O, while at high FCR the assemblage of a large anode area might also prevent its corrosion (Dou *et al.* 2010). Therefore, an excessively low or high FCR was unfavorable for the removal of phosphonate. The proper FCR would provide enough contact area ratios of anode to cathode, which was a prerequisite to achieve the optimal phosphonate removal (Liu *et al.* 2007; Ju & Hu 2011).

Effect of temperature on phosphonate removal

The temperature of discharged CCW usually fluctuated in the range of 20–40 °C. The effect of temperature on phosphonate removal was investigated and illustrated in Figure 1(c). An obvious influence of temperature on phosphonate removal was observed as PR increased from 46.8% at 15 °C to 86.7% at 50 °C. Higher temperature resulted in more active molecules generated by Fe/C micro-electrolysis, and accelerated the degradation of phosphonate. Furthermore, the increase of temperature also promoted the sedimentation of orthophosphate, which was in agreement with findings in previous studies for phosphorus removal by steel slag (Barca *et al.* 2012).

Response surface analysis

Development of regression model equation

Box–Behnken experimental design was used to develop correlation between experimental factors and removal efficiency. The complete design matrix and the response value obtained from the experimental results are shown in Table 1. The PR was found to range from 59.5% to 93.0%.

The relationship of the experimental results obtained from Box–Behnken experimental design and the input parameters was fitted by a second-order polynomial model with interaction terms. The final empirical model obtained in terms of coded factors is given below:

$$Y = 84.02 + 5.01X_1 + 4.59X_2 + 8.13X_3 - 1.19X_1X_2 - 8.17X_1X_3 - 3.53X_2X_3 + 2.78X_1^2 - 5.20X_2^2 + 2.07X_3^2 \quad (3)$$

The quality of the developed model was evaluated by the coefficient of determination. For Equation (3), the coefficient of determination (R^2) and adjusted-R^2 value were 0.9243 and 0.8271, respectively, which implied a high correlation between the experimental and the predicted values.

Analysis of variance

The results of the quadratic model in the form of analysis of variance (ANOVA) for PR are listed in Table 2. The sum of

Table 2 | Significance of quadratic model coefficients and variance analysis

Source	Sum of squares	d.f.	Mean square	*F*-value	*p*-value
Model	1382.37	9	153.60	9.50	0.0036
X_1	200.99	1	200.99	13.43	0.0096
X_2	168.78	1	168.82	10.44	0.0144
X_3	528.91	1	528.91	32.72	0.0007
$X_1 \times X_2$	5.64	1	5.64	0.35	0.5732
$X_1 \times X_3$	266.86	1	266.86	16.51	0.0048
$X_2 \times X_3$	49.96	1	49.96	3.09	0.1221
X_1^2	32.61	1	32.61	2.02	0.1985
X_2^2	114.04	1	114.04	7.06	0.0326
X_3^2	18.07	1	18.07	1.12	0.3255
Residual	113.14	7	16.16	–	–
Lack of fit	91.67	3	30.56	5.69	0.0631
Pure error	21.47	4	5.37	–	–
Cor total	1495.52	16	–	–	–

squares implies its importance in the model, and the significance of the corresponding parameters increases with the enhancement of the sum of squares. According to Table 2, the sum of squares was 528.91 for X_3, 200.99 for X_1 and 168.78 for X_2, respectively. This indicated that temperature was more influential than pH and FCR. Moreover, the *F*-values and associated *p*-values were used to conclude the order of the model; the large *F*-values suggest that most of the variation in the response can be explained by the quadratic model. The associated *p*-value is used to estimate whether the *F*-value was large enough to indicate statistical significance. The *p*-values lower than 0.05 indicate that the model is statistically significant (Segurola *et al.* 1999). In this case, X_1, X_2, X_3, $X_1 \times X_3$, and X_2^2 were significant model terms. The model *F*-value of 9.50 with a low associated *p*-value of 0.0036 indicated that the model terms were significant, too. 'Adequate precision' measures the signal-to-noise ratio and a ratio greater than 4 is desirable. The adequate precision in this case of 11.523 indicated an adequate signal and this model can be used to navigate the design space (Zhang *et al.* 2011). Simultaneously, the 'lack of fit *F*-value' of 5.69 (*p*-value = 0.0631) implied that the lack of fit was not significant, which also showed the model adequately described the data.

Three-dimensional (3D) plots were used to investigate the optimal levels and nonlinear interactions between the variables. The 3D plots of the response variable for experimental factors are shown in Figure 2.

Figure 2(a) shows that PR increased with the increase of pH and temperature, and the maximum value was achieved at pH of 7.0 and temperature of 45 °C. It was observed that the nonlinear interaction between pH and temperature was weakened as these two factors increased; that is, when one factor was beneficial for phosphorus removal, further increasing of the other factor would result in less improvement on removal efficiency compared to changing one factor individually and sometimes even decreasing the PR. The depth of color on the surface plot illustrated that the sensitivity of phosphonate removal to temperature was higher than to pH.

Figure 2(b) illustrates the interaction effect of pH and FCR on the PR. U-shape plot suggested that a suitable FCR would benefit PR. As shown in Figure 2(b), the PR

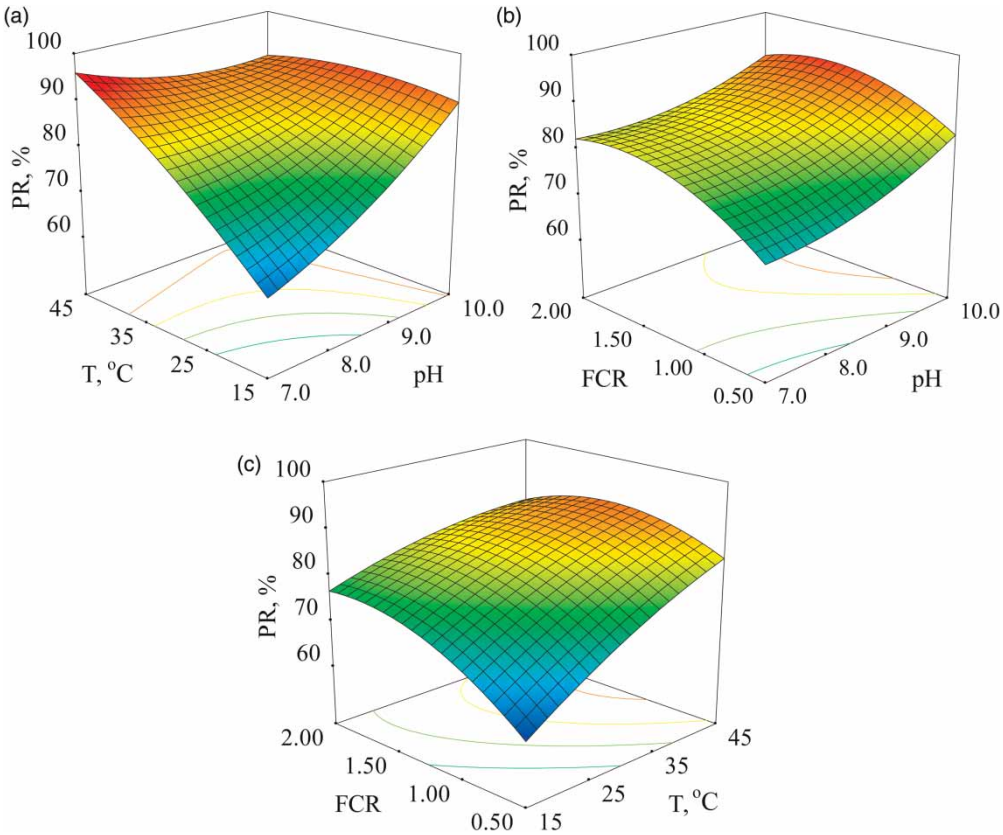

Figure 2 | 3D response surface plots for combined effects on the phosphonate removal from discharged CCW. (a) pH and temperature, FCR = 1.25; (b) pH and FCR, $T = 30$ °C; (c) temperature and FCR, pH = 8.5.

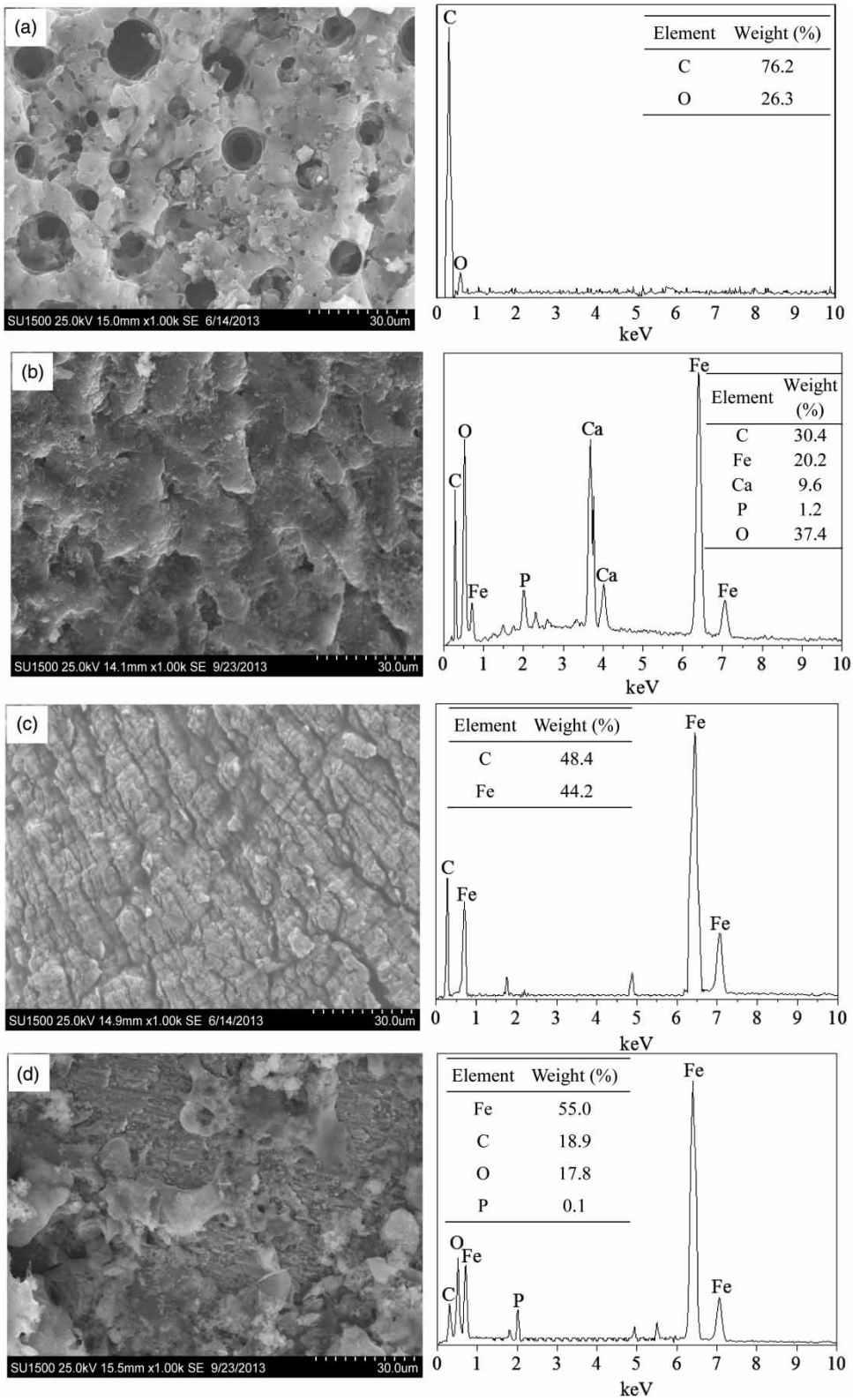

Figure 3 | SEM images and EDS patterns of AC/iron before (a), (c) and after (b), (d) experiment.

value was lower both at lower and higher FCR, and increased with an increase of pH. Phosphonate removal by Fe/C micro-electrolysis was favored in the range of pH of 9.4–10.0 and FCR of 1.1–1.9.

The interaction effect of temperature and FCR on PR is shown in Figure 2(c), and the minimum PR appeared at temperature of 15 °C and FCR of 0.5. From Figure 2(c), we could also concluded that the influence of temperature on phosphonate removal was more significant than FCR.

Model adequacy checking and optimal conditions

The predicted optimal results for phosphonate removal were obtained using the reaction temperature of 45 °C, FCR of 1.25 and pH of 7.0, resulting in 95.0% (with 95% confidence intervals of 88–103%) of PR for initial TP of 2.46 mg/L. To verify the model adequacy, these optimum values were checked experimentally, which resulted in 93.9 ± 1.0% of PR by Fe/C micro-electrolysis. The good correlation between these two results verified the validity of the response model and the existence of an optimal point.

Fe/C micro-electrolysis mechanism of phosphonate removal

The surface morphologies of iron and AC before and after reaction were compared by SEM and EDS analysis, and sample images are illustrated in Figure 3. Figure 3(a) shows that the surface of AC before the experiment was porous, which was in favor of adsorption. After the micro-electrolysis experiment, the pores disappeared and the surface was covered by scaly materials (Figure 3(b)) that contained Fe, O and P elements. This result confirmed that the ferro-phosphorus compounds precipitated on the surface of AC. Furthermore, element Ca was also observed on the surface of AC, and probably originated from the degradation of Ca–phosphonate complexes by Fe/C micro-electrolysis.

Figure 3(c) shows that before the experiment, the surface of iron was rough and accompanied with cracks, which could augment the reaction area and favor accretion of sediments and absorption of pollutant from the solution. After the experiment, the surface of iron had many scattered overlapping lumps (Figure 3(d)). The major elements on the surface of iron were Fe, C and O, but the percentage of P (0.1%) was significantly lower than that on the surface of AC (Figure 3(b)).

According to the experimental results, the main mechanism of phosphonate removal by Fe/C micro-electrolysis appeared to be composed of several primary consecutive reactive phases, as shown in Figure 4.

- Fe/C micro-electrolysis: release of Fe^{2+} and H_2O_2, [H] (in acid condition) or [OH] (in alkaline condition) to the solution (Cheng *et al.* 2007; Yang *et al.* 2009; Zhou *et al.* 2011).
- Phosphonate degradation: C-P bond of HEDP is broken by [H] (in acid condition), [OH] (in alkaline condition) and Fe^{3+}, and then orthophosphate is released to the solution. A supposed phosphonate degradation pathway is shown in Equation (4).

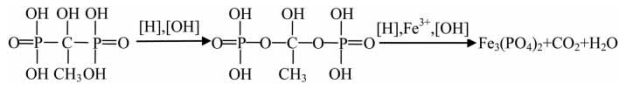

(4)

- The Ca–HEDP complex in the discharged CCW could also be degraded to release calcium ion to the solution.
- Iron precipitation: precipitation of Fe/C micro-electrolysis products, i.e., PO_4^{3-}, OH^-, Ca^{2+} and Fe^{3+}.

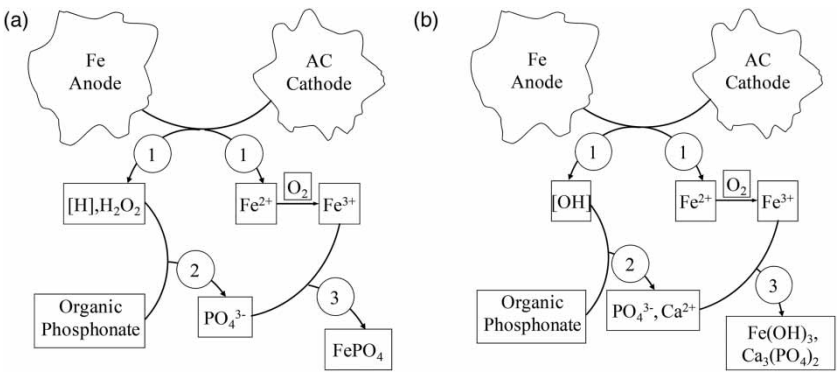

Figure 4 | Supposed process of phosphonate removal from discharged CCW. (a) Acid condition. (b) Alkaline condition.

- Flocculation of phosphorus: organic and inorganic phosphorus flocculated or absorbed by $Fe(OH)_3$ (in alkaline condition) (Figure 4(b)).

CONCLUSIONS

This study showed that Fe/C micro-electrolysis is efficient for phosphonate removal from discharged CCW. The phosphonate removal efficiency depended on initial pH, FCR and temperature. The effect of influencing factors on phosphonate removal was optimized using RSM. The quadratic model of phosphonate removal was obtained with satisfactory degrees of fitness. The optimum conditions with PR of 95% were obtained at pH 7.0, FCR of 1.25, and temperature of 45 °C. It was found that the phosphonate complex was degraded to orthophosphate and calcium by Fe/C micro-electrolysis, and then the orthophosphate was precipitated by released ferric and calcium ions to achieve phosphorus removal.

ACKNOWLEDGEMENT

This work was financially supported by the Key Project of Shanghai Science and Technology Committee (12250500900).

REFERENCES

Akyol, E., Öner, M., Barouda, E. & Demadis, K. D. 2009 Systematic structural determinants of the effects of tetraphosphonates on gypsum crystallization. *Cryst. Growth Des.* **9** (12), 5145–5154.

Barca, C., Troesch, S., Meyer, D., Drissen, P., Andrès, Y. & Chazarenc, F. 2012 Steel slag filters to upgrade phosphorus removal in constructed wetlands: two years of field experiments. *Environ. Sci. Technol.* **47** (1), 549–556.

Cheng, H., Xu, W., Liu, J., Wang, H., He, Y. & Chen, G. 2007 Pretreatment of wastewater from triazine manufacturing by coagulation, electrolysis, and internal microelectrolysis. *J. Hazard. Mater.* **146** (1), 385–392.

Chinese NEPA 2012 *Water and Wastewater Monitoring Methods*. Chinese Environmental Science Publishing House, Beijing, China.

Demadis, K. D., Mantzaridis, C. & Lykoudis, P. 2006 Effects of structural differences on metallic corrosion inhibition by metal-polyphosphonate thin films. *Ind. Eng. Chem. Res.* **45** (23), 7795–7800.

Demadis, K. D., Barouda, E., Raptis, R. G. & Zhao, H. 2008 Metal tetraphosphonate "wires" and their corrosion inhibiting passive films. *Inorg. Chem.* **48** (3), 819–821.

Dou, X., Li, R., Zhao, B. & Liang, W. 2010 Arsenate removal from water by zero-valent iron/activated carbon galvanic couples. *J. Hazard. Mater.* **182** (1), 108–114.

Guo, X., Cai, Y., Wei, Z., Hou, H., Yang, X. & Wang, Z. 2013 Treatment of diazo dye C.I. Reactive Black 5 in aqueous solution by combined process of interior microelectrolysis and ozonation. *Water Sci. Technol.* **67** (8), 1880–1885.

Ju, F. & Hu, Y. 2011 Removal of EDTA-chelated copper from aqueous solution by interior microelectrolysis. *Sep. Purif. Technol.* **78** (1), 33–41.

Kenny, J. F., Barber, N. L., Hutson, S. S., Linsey, K. S., Lovelace, J. K. & Maupin, M. A. 2009 *Estimated Use of Water in the United States in 2005*. US Geological Survey Reston, Reston, Virginia, USA.

Le, C., Zha, Y., Li, Y., Sun, D., Lu, H. & Yin, B. 2010 Eutrophication of lake waters in China: cost, causes, and control. *Environ. Manag.* **45** (4), 662–668.

Le, C., Wu, J. H., Li, P., Wang, X., Zhu, N. W., Wu, P. X. & Yang, B. 2011 Decolorization of anthraquinone dye Reactive Blue 19 by the combination of persulfate and zero-valent iron. *Water Sci. Technol.* **64** (3), 754–759.

Liang, B., Yao, Q., Cheng, H., Gao, S., Kong, F., Cui, D., Guo, Y., Ren, N. & Wang, A. 2012 Enhanced degradation of azo dye alizarin yellow R in a combined process of iron–carbon microelectrolysis and aerobic bio-contact oxidation. *Environ. Sci. Pollut. Res.* **19** (5), 1385–1391.

Liu, H., Li, G., Qu, J. & Liu, H. 2007 Degradation of azo dye Acid Orange 7 in water by Fe^0/granular activated carbon system in the presence of ultrasound. *J. Hazard. Mater.* **144** (1), 180–186.

Marín-Cruz, J., Cabrera-Sierra, R., Pech-Canul, M. & González, I. 2007 EIS characterization of the evolution of calcium carbonate scaling in cooling systems in presence of inhibitors. *J. Solid State Electrochem.* **11** (9), 1245–1252.

Myers, R. H. & Anderson-Cook, C. M. 2009 *Response Surface Methodology: Process and Product Optimization Using Designed Experiments*. Wiley, Hoboken, New Jersey, USA.

Pan, F., Luo, Y., Zhang, L. R. & Fu, J. 2011 Degradation of Reactive Brilliant Red X-3B by zero-valent iron/activated carbon system in the presence of microwave irradiation. *Water Sci. Technol.* **64** (12), 2345–2351.

Segurola, J., Allen, N. S., Edge, M. & Mc Mahon, A. 1999 Design of eutectic photoinitiator blends for UV/visible curable acrylated printing inks and coatings. *Prog. Org. Coat.* **37** (1), 23–37.

Tripathi, P., Srivastava, V. C. & Kumar, A. 2009 Optimization of an azo dye batch adsorption parameters using Box–Behnken design. *Desalination* **249** (3), 1273–1279.

Wang, Y., Peng, Y. & Stephenson, T. 2009 Effect of influent nutrient ratios and hydraulic retention time (HRT) on simultaneous phosphorus and nitrogen removal in a two-sludge sequencing batch reactor process. *Bioresour. Technol.* **100** (14), 3506–3512.

Yang, X., Xue, Y. & Wang, W. 2009 Mechanism, kinetics and application studies on enhanced activated sludge by interior microelectrolysis. *Bioresour. Technol.* **100** (2), 649–653.

Zhang, T., Li, Q., Ding, L., Ren, H., Xu, K., Wu, Y. & Sheng, D. 2011 Modeling assessment for ammonium nitrogen recovery from wastewater by chemical precipitation. *J. Environ. Sci.* **23** (6), 881–890.

Zhou, Y.-f., Liu, M. & Wu, Q. 2011 Water quality improvement of a lagoon containing mixed chemical industrial wastewater by micro-electrolysis-contact oxidization. *J. Zhejiang Univ. Sci. A* **12** (5), 390–398.

First received 9 April 2014; accepted in revised form 16 May 2014. Available online 3 June 2014